

Experimental signals for a second resonance of the Brout-Englert-Higgs field

Maurizio Consoli

INFN-Sezione di Catania and CMS Collaboration

Conference in Honor of Yves Brihaye

Mons 2-3 June 2022

References:

M.C., L. Cosmai, Int. J. Mod. Phys. A **35** (2020) 2050103; hep-ph/2006.15378

M.C., L. Cosmai, Symmetry **12** (2020) 2037; doi:103390/sym12122037

M.C. , in Veltman Memorial Volume, Acta Phys. Pol. B **52** (2021) 763; hep-ph/2106.06543

M.C., L. Cosmai, arXiv:2111.08962v3 [hep-ph], accepted by Int. J. Mod. Phys. A

Abstract

- 1) Theoretical arguments + lattice simulations give motivations for a relatively narrow, second resonance of the Brout-Englert-Higgs field with mass

$$(M_H)^{\text{THEOR}} = 690 \pm 10 \text{ (stat)} \pm 20 \text{ (sys) GeV} \quad (*)$$

produced mainly via gluon-gluon Fusion (ggF)

- 2) The ATLAS 4-lepton events for invariant mass $M(4l) = 620 \div 740$ GeV, indicate an excess which can be interpreted as a new resonance of mass

$$(M_H)^{\text{EXP}} = 660 \div 680 \text{ GeV} \quad \text{consistently with } (*)$$

- 3) Moreover, the $m_h = 125$ GeV and the new $(M_H)^{\text{EXP}}$ are **correlated** as expected if the latter were indeed the second resonance of the Brout-Englert-Higgs field

- 4) Our basic **correlation** becomes a guiding-principle to trust in other (small) excesses which may be present in other final states. The issue could thus be settled now, with just the present data from the RUN2 of LHC

- 5) Miscellanea of other technical aspects: present CMS 4-lepton data, other final states (e.g. peak at 680 GeV in the ATLAS $\gamma\gamma$ events, more from CMS...), the $H \rightarrow \gamma\gamma$ decay puzzle (Gastmans-Wu-Wu & Todorov-Christova against the rest of the world), effect of a two-mass structure of the Brout-Englert-Higgs field on radiative corrections,

Presently accepted view of SSB as a 2-nd order phase transition:
the spectrum of the BEH field consists of a single narrow resonance of
mass **$m_h = 125 \text{ GeV}$**

At present, the excitation spectrum of the Higgs field is described in terms of a single narrow resonance of mass $m_h = 125 \text{ GeV}$ associated with the quadratic shape of the effective potential at its minimum. In a description of Spontaneous Symmetry Breaking (SSB) as a second-order phase transition, this point of view is well summarized in the review of the Particle Data Group [1] where the scalar potential is expressed as

$$V_{\text{PDG}}(\varphi) = -\frac{1}{2}m_{\text{PDG}}^2\varphi^2 + \frac{1}{4}\lambda_{\text{PDG}}\varphi^4 \quad (1)$$

By fixing $m_{\text{PDG}} \sim 88.8 \text{ GeV}$ and $\lambda_{\text{PDG}} \sim 0.13$, this has a minimum at $|\varphi| = \langle\Phi\rangle \sim 246 \text{ GeV}$ and a second derivative $V''_{\text{PDG}}(\langle\Phi\rangle) \equiv m_h^2 = (125 \text{ GeV})^2$.

However, not everybody agrees with this picture of SSB.
SSB could be a (weak) first-order phase transition

- **Gaussian quantization, O_N theory and the Goldstone theorem**

- **Y. Brihaye** & M. Consoli

- Il Nuovo Cimento A **94** (1986) p. 1–14.

- **Summary:**

A Gaussian variational principle for an O_N -invariant self-interacting theory is formulated. The conditions for spontaneous symmetry breaking and the limits of validity of the approximation are analysed in detail.

SSB in **cutoff Φ^4** \rightarrow weak first-order phase transition

P.H. Lundow and K. Markstroem, PRE 80(2009)031104; NPB 845(2011)120

picture below from S. Akiyama et al. PRD 100(2019)054510

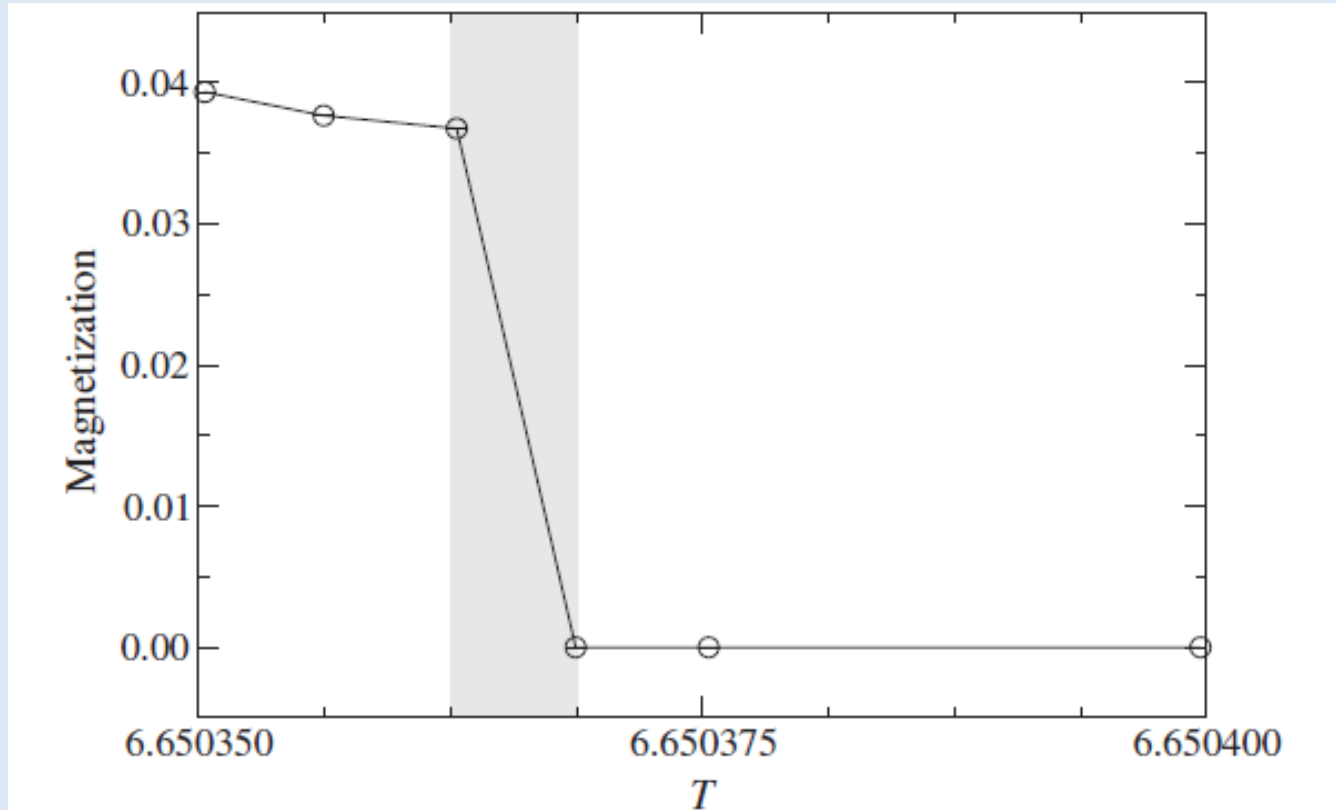
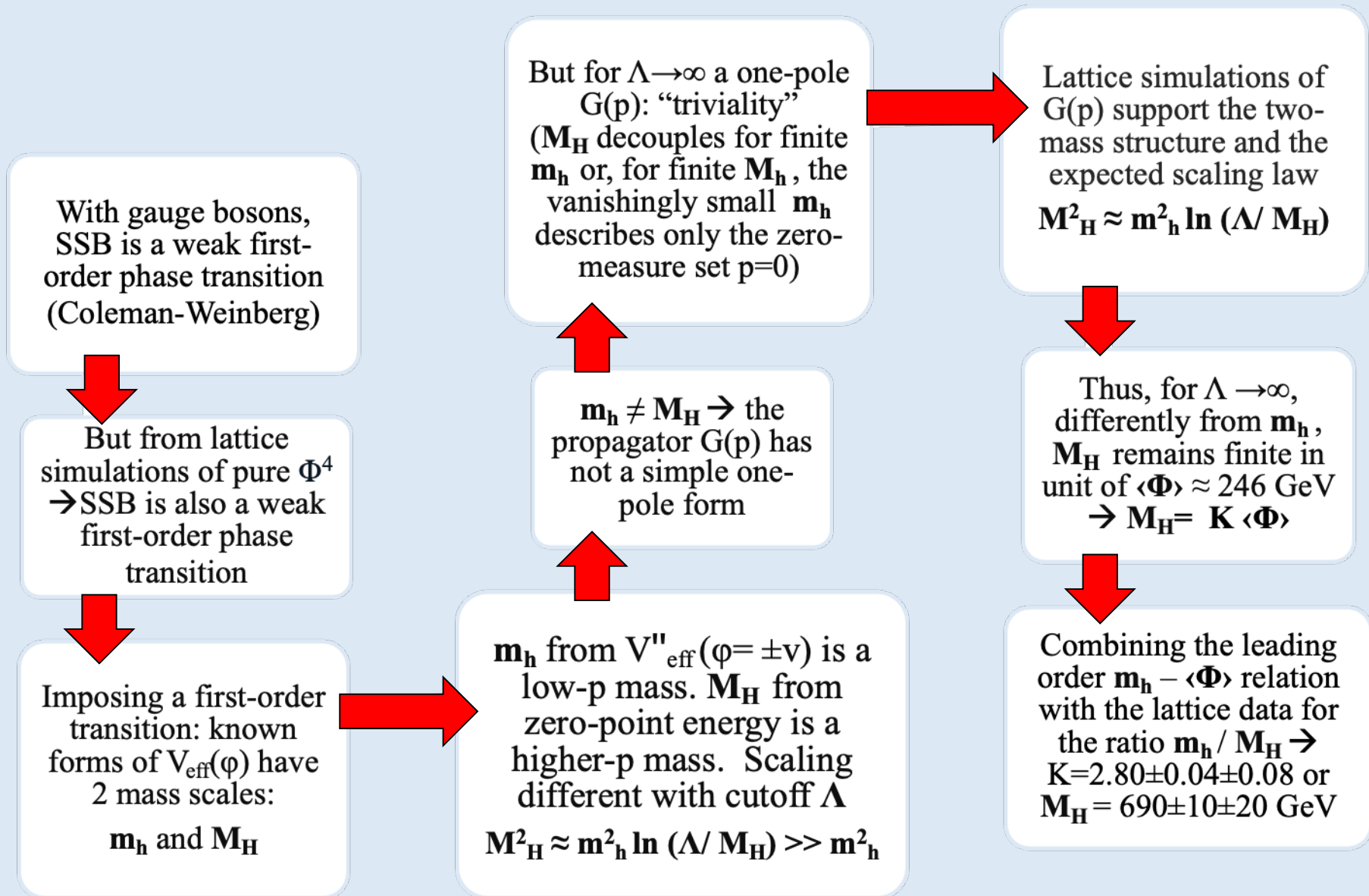


FIG. 7. Spontaneous magnetization in the thermodynamic limit with $D_{\text{cut}} = 13$. Error bars, provided by extrapolation, are within symbols. $T_c(D_{\text{cut}} = 13)$ estimated by $X^{(n)}$ of Eq. (15) is within the gray band.

A new picture: a 700 GeV resonance of the BEH field \rightarrow SSB induced by the pure scalar sector (W,Z, top-quark irrelevant)



How to understand SSB as a 1st-order transition?

- With a physical mass in the symmetric $\langle \Phi \rangle = 0$ phase, can we understand the origin of SSB? In the presence of gauge bosons, this was shown long ago by Coleman and Weinberg. But in a pure Φ^4 ? Key observation: the interaction is not purely repulsive:

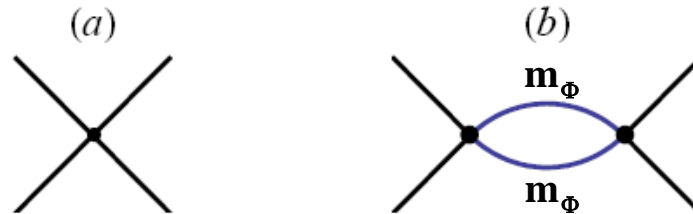


Figure 1: (a) The fundamental interaction. (b) The “fish” diagram, which induces a long-range interaction.

- Diagram (a) gives the repulsive contact potential $\delta^{(3)}(\mathbf{r})$
- Diagram (b) renormalizes the term $\delta^{(3)}(\mathbf{r})$ and introduces an attractive tail

$$-\frac{\lambda^2}{r^3} e^{-2m_\Phi r}$$

that becomes long-range when $m_\Phi \rightarrow 0$ (SSB)

Higher orders just renormalize symmetrically the strength of the two basic effects

$$“\lambda\Phi^4” = \text{tree} + \text{one-loop} + \text{higher orders}$$



$$“\lambda\Phi^4” = \left[\text{tree} + \text{uv - finite one-loop} \right] + \text{uv - divergent one-loop} + \text{higher orders}$$

SSB as a (weak) first-order phase transition

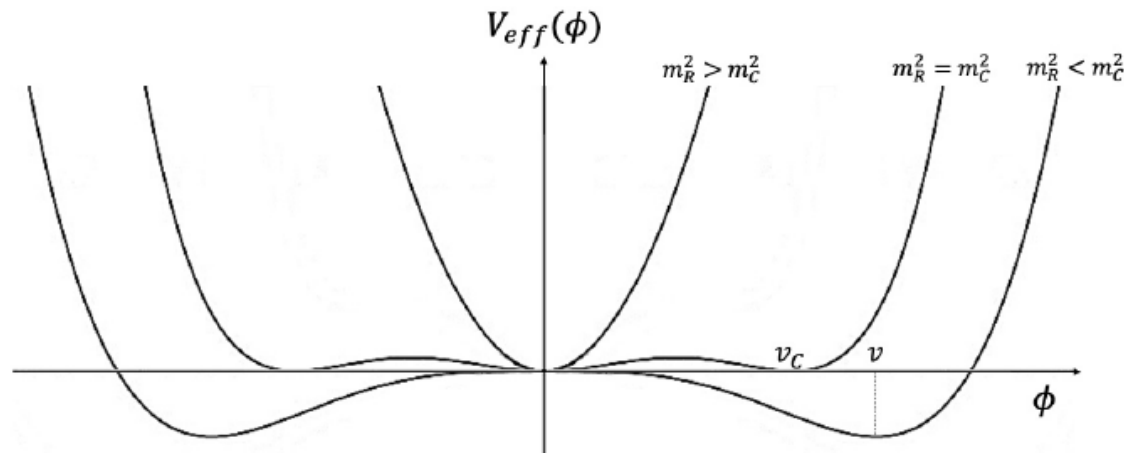


Figure 1: A *schematic profile of the effective potential where SSB is a 1st-order phase transition.*

Physical implications

- Physical interpretation \rightarrow SSB, as (weak) first-order phase transition, is a **true condensation phenomenon**
- Namely, the condensation process of quanta which have a **physical mass**
- What about the mass spectrum of the broken-symmetry phase? Could it differ from what naively expected?
- Look at the resulting structure of the effective potential

Simplest approximations to (pure) Φ^4 where SSB is weakly 1st-order:

1-loop and Gaussian potential \rightarrow 2 mass scales:

m_h from quadratic shape of $V_{\text{eff}}(\varphi = \pm v)$ and M_H from zero-point energy

By introducing the mass-squared parameter $M^2(\varphi) \equiv \frac{1}{2}\lambda\varphi^2$, the 1-loop potential can be expressed as a classical background + zero-point energy of a particle with mass $M(\varphi)$, i.e.

$$V_{1\text{-loop}}(\varphi) = \frac{\lambda\varphi^4}{4!} - \frac{M^4(\varphi)}{64\pi^2} \ln \frac{\Lambda_s^2 \sqrt{e}}{M^2(\varphi)} \quad (9)$$

Thus, non-trivial minima of $V_{\text{eff}}(\varphi)$ occur at those points $\varphi = \pm v$ where

$$M_H^2 = \frac{\lambda v^2}{2} = \Lambda_s^2 \exp\left(-\frac{32\pi^2}{3\lambda}\right) \quad (10)$$

with a quadratic shape

$$m_h^2 \equiv V''_{1\text{-loop}}(\pm v) = \frac{\lambda^2 v^2}{32\pi^2} = \frac{\lambda}{16\pi^2} M_H^2 \sim \frac{M_H^2}{L} \ll M_H^2 \quad (11)$$

where $L \equiv \ln \frac{\Lambda_s}{M_h}$. Notice that the energy density depends on M_h and *not* on m_h , because

$$\mathcal{E}_{1\text{-loop}} = V_{1\text{-loop}}(\pm v) = -\frac{M_H^4}{128\pi^2} \quad (12)$$

therefore the critical temperature at which symmetry is restored, $k_B T_c \sim M_H$, and the stability of the broken phase depends on the larger M_H and not on the smaller m_h .

$$V_G(\varphi) = \frac{\hat{\lambda}\varphi^4}{4!} - \frac{\Omega^4(\varphi)}{64\pi^2} \ln \frac{\Lambda_s^2 \sqrt{e}}{\Omega^2(\varphi)}$$

$$\hat{\lambda} = \frac{\lambda}{1 + \frac{\lambda}{16\pi^2} \ln \frac{\Lambda_s}{\Omega(\varphi)}}$$

$$\Omega^2(\varphi) = \frac{\hat{\lambda}\varphi^2}{2}$$

$$M_H^2 = \Omega^2(v)$$

$$\mathcal{E}_G = V_G(\pm v) = -\frac{M_H^4}{128\pi^2}$$

In both approximations

$$m_h^2 \equiv V''_{\text{eff}}(\pm v) \sim \frac{M_H^2}{L} \ll M_H^2$$


$m_h \neq M_H \rightarrow$ propagator $G(p)$ has not a single-pole structure

m_h^2 , being $V''_{\text{eff}}(\varphi)$ at the minimum, is directly the 2-point, self-energy function $|\Pi(p=0)|$.

On the other hand, the Zero-Point Energy (ZPE) is (one-half of) the trace of the logarithm of the inverse propagator $G^{-1}(p) = (p^2 - \Pi(p))$. After subtracting constant terms and quadratic divergences, matching the 1-loop zero-point energy at the minimum gives the relation

$$ZPE \sim -\frac{1}{4} \int_{p_{\min}}^{p_{\max}} \frac{d^4 p}{(2\pi)^4} \frac{\Pi^2(p)}{p^4} \sim -\frac{\langle \Pi^2(p) \rangle}{64\pi^2} \ln \frac{p_{\max}^2}{p_{\min}^2} \sim -\frac{M_H^4}{64\pi^2} \ln \frac{\Lambda_s^2}{M_H^2} \quad (3)$$

This shows that M_H^2 effectively refers to some average value $|\langle \Pi(p) \rangle|$ at larger p^2 .

 Therefore, if $m_h \neq M_H$, there must be a non-trivial momentum dependence of $\Pi(p)$



Check with lattice simulations of the scalar propagator.

Lattice simulations of the scalar propagator



ELSEVIER

Available online at www.sciencedirect.com

SCIENCE @ DIRECT®

Nuclear Physics B 729 [FS] (2005) 542–557

NUCLEAR
PHYSICS B

Comparison of perturbative RG theory with lattice data for the 4d Ising model

P.M. Stevenson

$$S = \sum_x \left[-2\kappa \sum_{\mu=1}^4 \phi(x) \phi(x + \hat{\mu}) + \phi(x)^2 + \lambda (\phi(x)^2 - 1)^2 \right], \quad (1)$$

which is equivalent to the more traditional expression

$$S = \sum_x \left[\frac{1}{2} \sum_{\mu=1}^4 (\partial_{\mu} \phi_0(x))^2 + \frac{1}{2} m_0^2 \phi_0(x)^2 + \frac{g_0}{4!} \phi_0^4 \right], \quad (2)$$

where $\partial_{\mu} \phi_0(x) = \phi_0(x + \hat{\mu}) - \phi_0(x)$. The translation between the two formulations is given by

$$\phi_0 = \sqrt{2\kappa} \phi, \quad m_0^2 = \frac{(1 - 2\lambda)}{\kappa} - 8, \quad g_0 = \frac{6\lambda}{\kappa^2}. \quad (3)$$

Stevenson's analysis of the lattice propagator

(data from Balog, Duncan, Willey, Niedermeyer, Weisz NPB714(2005)256)

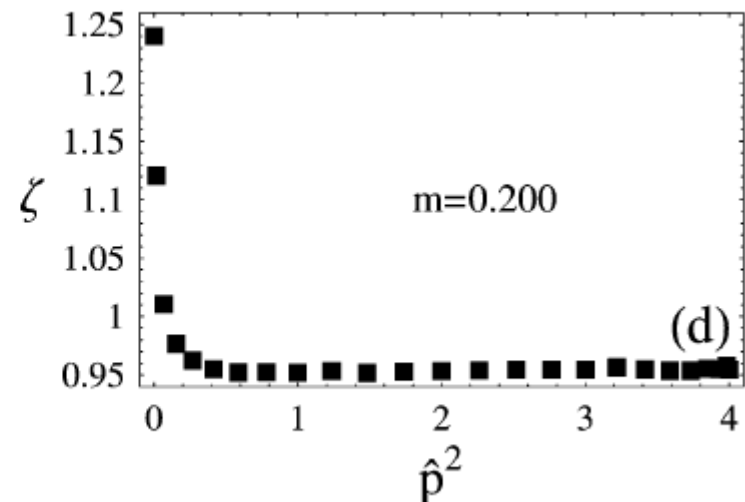
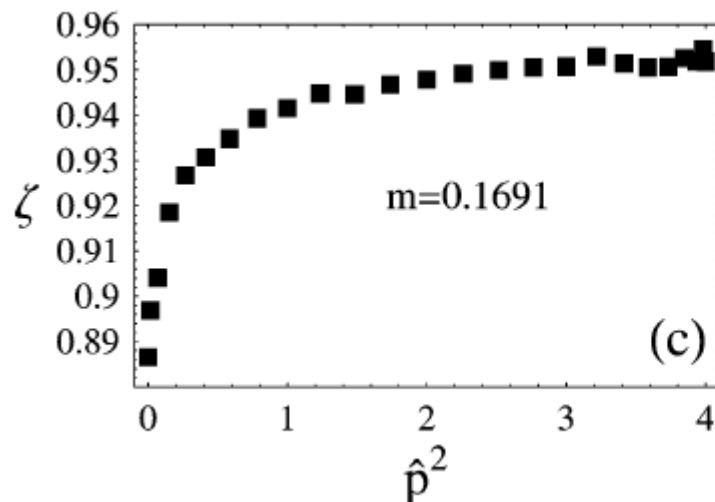
For $\kappa=0.0751$ in the broken phase, he reports the rescaled propagator.

$$\zeta \equiv (\hat{p}^2 + m^2)G(p)$$

Standard one-pole propagator $\rightarrow \zeta$ has a flat profile

Left: re-scaling with the mass 0.1691 from the $p=0$ limit

Right: re-scaling with the mass giving a flat profile at larger p^2



Lattice Checks

(M.C. and Leonardo Cosmai, Int. J. Mod. Phys. A35 (2020) 2050103; hep-ph/2006.15378

- A consistency check: no two-mass structure in the symmetric phase

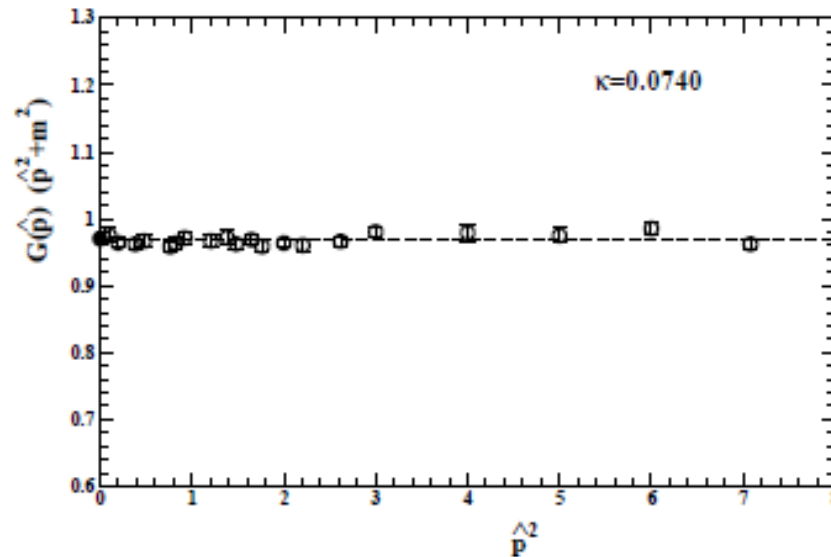
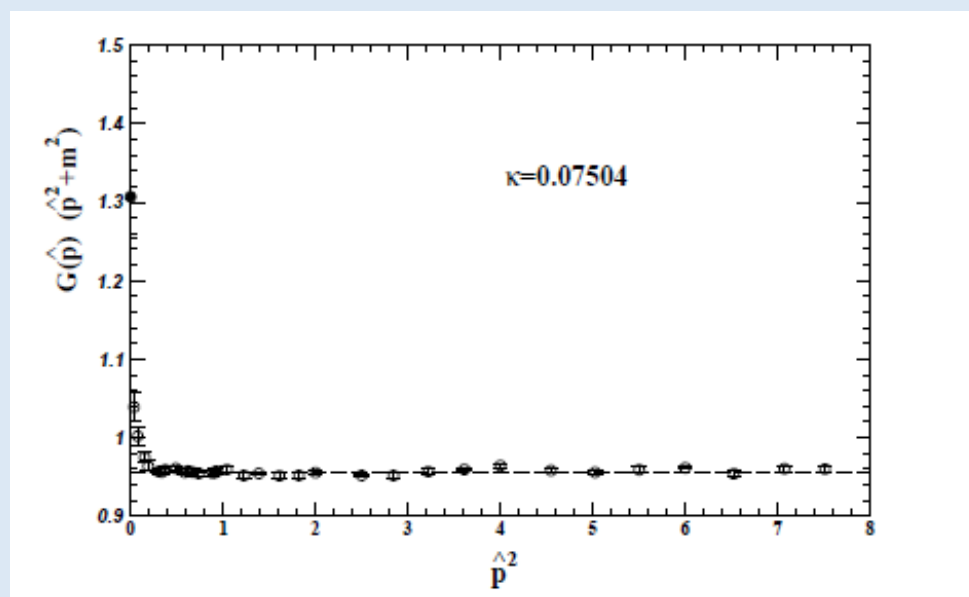
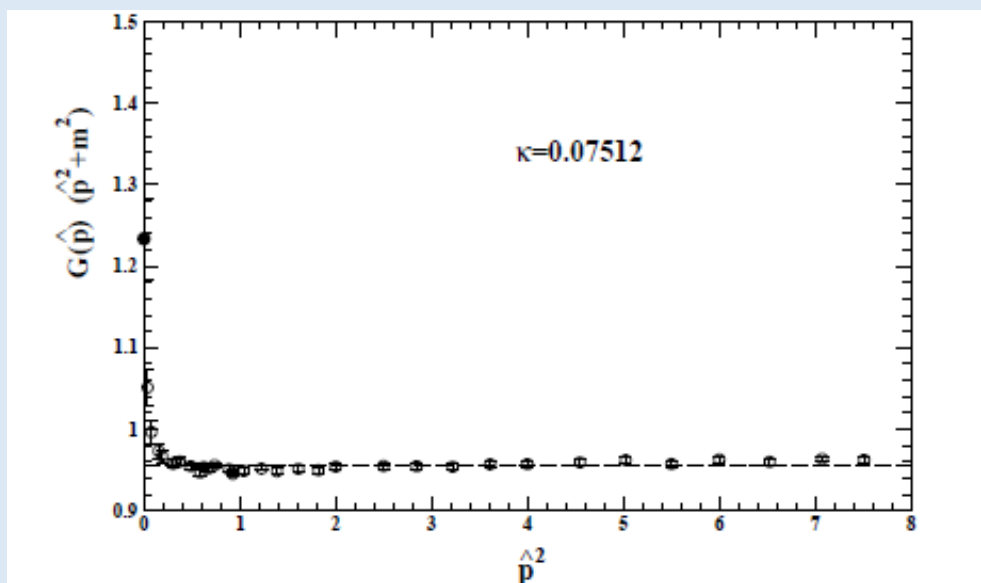


Figure 1: *The lattice data of ref.[8] for the re-scaled propagator in the symmetric phase at $\kappa = 0.074$ as a function of the square lattice momentum \hat{p}^2 . The fitted mass from high \hat{p}^2 , $m_{\text{latt}} = 0.2141(28)$, describes well the data down to $\hat{p} = 0$. The dashed line indicates the value of $Z_{\text{prop}} = 0.9682(23)$ and the $\hat{p} = 0$ point is $2\kappa\chi m_{\text{latt}}^2 = 0.9702(91)$.*

Lattice propagator in the broken phase



Propagator on a 76^4 lattice: **2** flat ranges \rightarrow **2** mass-shell regions

(M.C. and L.Cosmai, IJMP A35 (2020) 2050103; hep-ph/2006.15378)

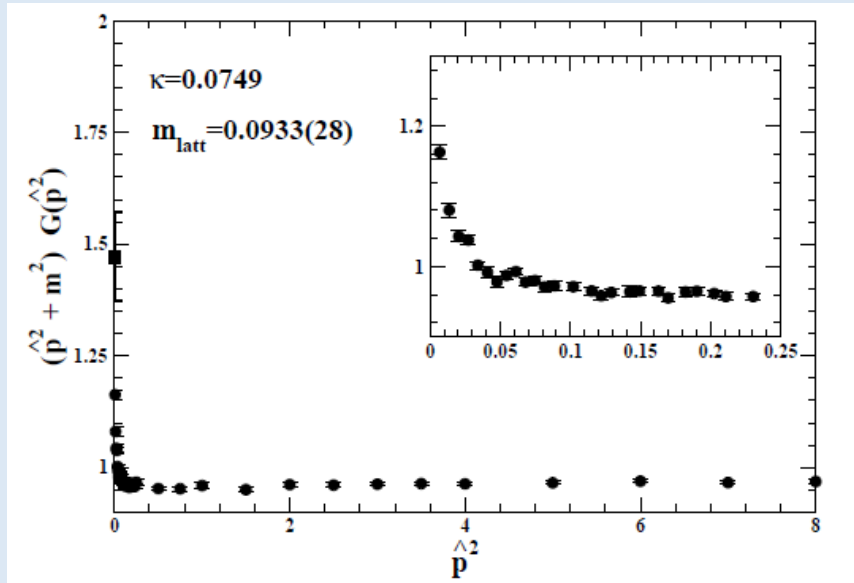


Figure 2: The propagator data of ref.[8], for $\kappa = 0.0749$, rescaled with the lattice mass $M_H \equiv m_{\text{latt}} = 0.0933(28)$ obtained from the fit to all data with $\hat{p}^2 > 0.1$. The peak at $p = 0$ is $M_H^2/m_h^2 = 1.47(9)$ as computed from the fitted M_H and $m_h = (2\kappa\chi)^{-1/2} = 0.0769(8)$.

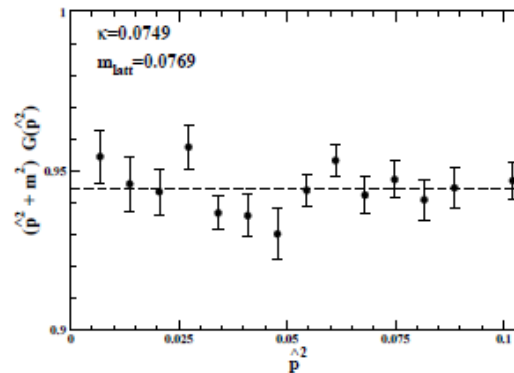


Figure 3: The propagator data of ref.[8] at $\kappa = 0.0749$ for $\hat{p}^2 < 0.1$. The lattice mass used here for the rescaling was fixed at the value $m_h = (2\kappa\chi)^{-1/2} = 0.0769(8)$.

Two-mass structure of the lattice propagator

Then, by computing m_h^2 from the $p \rightarrow 0$ limit of $G(p)$ and M_H^2 from its behaviour at higher p^2 , the lattice data are consistent with a transition between two different regimes and were well described in the full momentum region by the model form

$$G(p) \sim \frac{1 - I(p)}{2} \frac{1}{p^2 + m_h^2} + \frac{1 + I(p)}{2} \frac{1}{p^2 + M_H^2} \quad (29)$$

with an interpolating function $I(p)$ which depends on an intermediate momentum scale p_0 and tends to $+1$ for large $p^2 \gg p_0^2$ and to -1 when $p^2 \rightarrow 0$. Most notably, the lattice data were also consistent with the expected increasing logarithmic trend $M_H^2 \sim m_h^2 \ln(\Lambda_s/M_H)$ when approaching the continuum limit.

The proportionality relation between M_H and $\langle\Phi\rangle \approx 246 \text{ GeV}$

Since, differently from m_h , the larger M_H would remain finite in units of the weak scale $\langle\Phi\rangle \sim 246.2 \text{ GeV}$ for an infinite ultraviolet cutoff, one can derive their proportionality relation. To this end, let us express M_H^2 in terms of $m_h^2 L$ through some constant c_2 , say

$$M_H^2 = m_h^2 L \cdot (c_2)^{-1} \quad (5)$$

and replace the leading-order estimate $\lambda \sim 16\pi^2/(3L)$ in the relation $\lambda = 3m_h^2/\langle\Phi\rangle^2$. Then M_H and $\langle\Phi\rangle$ are related through a cutoff-independent constant K

$$M_H = K \langle\Phi\rangle \quad (6)$$

with $K \sim (4\pi/3) \cdot (c_2)^{-1/2}$.

Estimating M_H from lattice simulations

Table 5: The values of M_H , as obtained from a direct fit to the higher-momentum propagator data. The two entries at $\kappa = 0.0749$, from our new simulations on a 76^4 lattice, refer to higher-momentum fits for $\hat{p}^2 > 0.1$ and $\hat{p}^2 > 0.2$ respectively. In the last column we report the combination $(c_2)^{-1/2} \equiv M_H \cdot (m_h)^{-1} \cdot [\ln(\Lambda_s/m_{M_H})]^{-1/2}$.

κ	M_H	$(m_h)^{-1}$	$[\ln(\Lambda_s/M_H)]^{-1/2}$	$(c_2)^{-1/2}$
0.07512	0.2062(41)	5.386(23)	0.606(2)	0.673(14)
0.0751	~ 0.200	5.568(16)	~ 0.603	~ 0.671
0.07504	0.1723(34)	6.636(32)	0.587(2)	0.671(14)
0.0749	0.0933(28)	13.00(14)	0.533(2)	0.647(20)
0.0749	0.100(6)	13.00(14)	0.538(4)	0.699(42)

- $(c_2)^{-1/2} = 0.67 \pm 0.01 \text{ (stat)} \pm 0.02 \text{ (sys)}$
- $K \equiv (4/3)\pi(c_2)^{-1/2} = 2.81 \pm 0.04 \text{ (stat)} \pm 0.08 \text{ (sys)}$
- $M_H = K \langle \Phi \rangle = 690 \pm 10 \text{ (stat)} \pm 20 \text{ (sys) GeV}$

Basic phenomenology of the (hypothetical) new 700 GeV resonance

With a mass $M_H = K\langle\Phi\rangle \approx 700$ GeV one usually expects strong interactions governed by the large coupling $\lambda_0=3K^2$

This reflects tree-level calculations in the unitary gauge where $W_L W_L$ scattering is like $\chi\chi$ scattering with the same contact coupling at all momentum scales

But beyond tree-level, in $\chi\chi$ scattering the contact coupling $\lambda_0=3K^2$, at a scale Λ , becomes, at a scale μ , the coupling $\lambda(\mu)$ whose evolution is determined by the β -function

This is also consistent with the “triviality” of Φ^4 : the constant $3K^2$ **cannot** be a measure of observable interactions. For $\mu \approx M_H$

$$\lambda(M_H) = 3K^2(m_h/M_H)^2 \approx G_F m_h^2$$

Therefore, one finds

$$A(W_L W_L \rightarrow W_L W_L) = A(\chi\chi \rightarrow \chi\chi)[1+O(g^2)] \approx \lambda(\mu)$$

Namely, at the scale μ ,

$$A(\chi\chi \rightarrow \chi\chi) \approx \lambda(\mu)$$
 with $\lambda(\mu) \approx 1/L$ and $L = \ln(\Lambda/\mu)$. By the Equivalence Theorem, the same applies to $W_L W_L \rightarrow W_L W_L$

The same holds true for other observable quantities of the scalar sector, in particular for the heavy M_H width

$$\Gamma(M_h \rightarrow W_L W_L) \approx \frac{M_h}{M_H} (G_F m_h^2)$$

The heavy M_H if it exists, would be a relative narrow resonance

With a relatively small decay width into longitudinal W's, main M_H -production at LHC via Gluon-Gluon-Fusion

Basic phenomenology of the heavy resonance. I

A heavy Higgs resonance H , with mass $M_H = K\langle\Phi\rangle \sim 700$ GeV, is usually believed to be a broad resonance due to the strong interactions in the scalar sector. This view derives from the original Lee-Quigg-Tacker calculation in the unitary gauge showing that, with a mass M_H in the scalar propagator, high-energy $W_L W_L$ scattering is indeed similar to $\chi\chi$ Goldstone boson scattering with a large contact coupling $\lambda_0 = 3K^2$. The same coupling would also enter the $H \rightarrow W_L W_L$ decay width.

However, by accepting the “triviality” of Φ^4 theories in 4D, the Λ –independent combination $3M_H^2/\langle\Phi\rangle^2 = 3K^2$ *cannot* represent a coupling entering observable processes. Indeed, the constant $3K^2$ is basically different from the coupling λ governed by the β –function

$$\ln \frac{\mu}{\Lambda} = \int_{\lambda_0}^{\lambda} \frac{dx}{\beta(x)} \quad (8)$$

For $\beta(x) = 3x^2/(16\pi^2) + O(x^3)$, whatever the contact coupling λ_0 at the asymptotically large Λ , at finite scales $\mu \sim M_H$ this gives $\lambda \sim 16\pi^2/(3L)$ with $L = \ln(\Lambda/M_H)$.

Basic phenomenology of the heavy resonance. II

Therefore, to find the $W_L W_L$ scattering amplitude at some scale μ , one should improve on the Lee-Quigg-Tacker calculation and first use the β -function to re-sum the higher-order effects in $\chi\chi$ scattering

$$A(\chi\chi \rightarrow \chi\chi) \Big|_{g_{\text{gauge}}=0} \sim \lambda \sim \frac{1}{\ln(\Lambda_s/\mu)} \quad (9)$$

and then use the Equivalence Theorem [18, 19, 20] which gives

$$A(W_L W_L \rightarrow W_L W_L) = [1 + O(g_{\text{gauge}}^2)] A(\chi\chi \rightarrow \chi\chi) \Big|_{g_{\text{gauge}}=0} = O(\lambda) \quad (10)$$

Thus the large coupling $\lambda_0 = 3K^2$ is actually replaced by the much smaller coupling

$$\lambda = \frac{3m_h^2}{\langle\Phi\rangle^2} = 3K^2 \frac{m_h^2}{M_H^2} \sim 1/L \quad (11)$$

M_H : heavy but relatively narrow resonance

(produced mainly by the gluon-gluon Fusion mechanism)

For the same reason, the conventional large width into longitudinal vector bosons computed with $\lambda_0 = 3K^2$, say $\Gamma^{\text{conv}}(H \rightarrow W_L W_L) \sim M_H^3 / \langle \Phi \rangle^2$, should instead be rescaled by $(\lambda/3K^2) = m_h^2/M_H^2$. This gives

$$\Gamma(H \rightarrow W_L W_L) \sim \frac{m_h^2}{M_H^2} \Gamma^{\text{conv}}(M_H \rightarrow W_L W_L) \sim M_H \frac{m_h^2}{\langle \Phi \rangle^2} \quad (12)$$

where M_H indicates the available phase space in the decay and $m_h^2/\langle \Phi \rangle^2$ the interaction strength. If the heavier state couples to longitudinal W's with the same typical strength of the low-mass state it would represent a relatively narrow resonance.

Due to the suppression of the conventional H-width into longitudinal W's and Z's, the relevant production mechanism in our picture is through the Gluon-Gluon Fusion (GGF) process. In fact, the other production through Vector-Boson Fusion (VBF) plays no role. The point is that the $VV \rightarrow H$ process (here $VV = W^+W^-, ZZ$) is the inverse of the $H \rightarrow VV$ decay so that $\sigma^{\text{VBF}}(pp \rightarrow H)$ can be expressed [26] as a convolution with the parton densities of the same Higgs resonance decay width. The importance given traditionally to VBF depends on the conventional large width into longitudinal W's and Z's computed with the $3K^2$ coupling. In our case, where this width is rescaled by the small ratio $(125/700)^2 \sim 0.032$, one finds $\sigma^{\text{VBF}}(pp \rightarrow H) \lesssim 10 \text{ fb}$ which can be safely neglected.

The widths $\Gamma(H \rightarrow WW)$ and $\Gamma(H \rightarrow ZZ)$ are much smaller than their conventional values. However, many new channels ...

- **$H \rightarrow hh$**
- **$H \rightarrow hhh$**
- **$H \rightarrow hWW$**
- **$H \rightarrow hZZ$**
- **....**
- **Hard to estimate the total width $\Gamma(H \rightarrow \text{all})$**
- **Hence: a test which does NOT require to know $\Gamma(H \rightarrow \text{all})$**

- **This is possible in the 4-lepton channel**

The process $pp \rightarrow H \rightarrow 4\text{-leptons}$

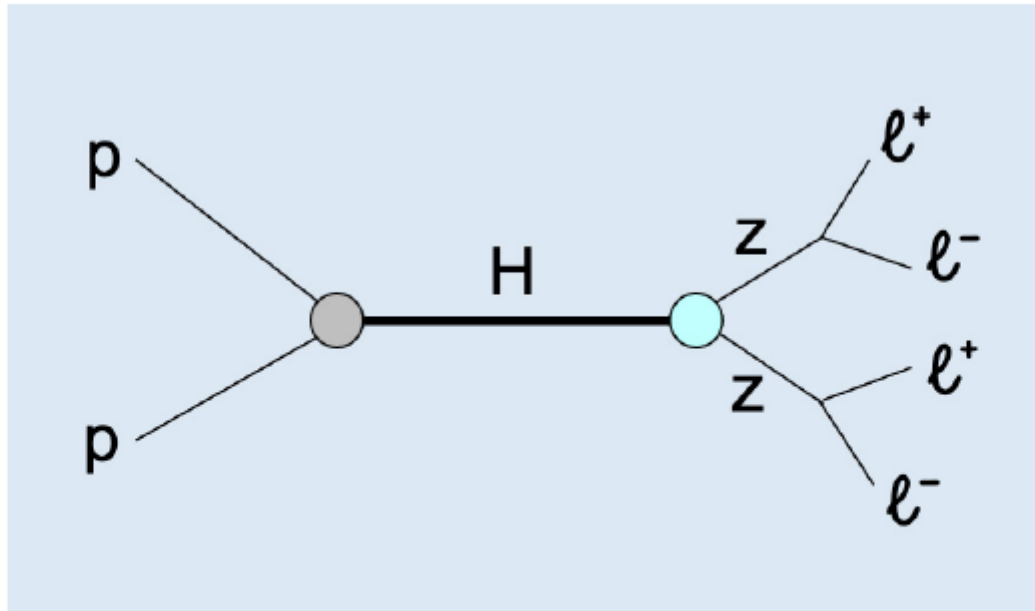


Figure 1: *The 4-lepton production through the chain $H \rightarrow ZZ \rightarrow 4l$.*

Phenomenology in the 4-lepton channel

- For $M_H \approx 700 \text{ GeV}$ the conventional $\Gamma(H \rightarrow ZZ)$ width is $G_F M_H^3 \approx 56.7 \text{ GeV}$ while here

$$\Gamma(H \rightarrow ZZ) \sim \frac{M_H}{700 \text{ GeV}} \cdot \frac{m_h^2}{(700 \text{ GeV})^2} 56.7 \text{ GeV} \quad (14)$$

Therefore, by defining $\gamma_H = \Gamma(H \rightarrow \text{all})/M_H$, we find a fraction

$$B(H \rightarrow ZZ) = \frac{\Gamma(H \rightarrow ZZ)}{\Gamma(H \rightarrow \text{all})} \sim \frac{1}{\gamma_H} \cdot \frac{56.7}{700} \cdot \frac{m_h^2}{(700 \text{ GeV})^2} \quad (15)$$

- For a relatively narrow resonance (whose virtuality effects should be small) approximate the cross section by a chain of on-shell branching ratios

$$\sigma_R(pp \rightarrow H \rightarrow 4l) \sim \sigma(pp \rightarrow H) \cdot B(H \rightarrow ZZ) \cdot 4B^2(Z \rightarrow l^+l^-) \quad (16)$$

- so that we find a $\gamma_H - \sigma_R$ correlation mainly determined by the low-mass m_h

$$\gamma_H \cdot \sigma_R(pp \rightarrow H \rightarrow 4l) \sim \sigma(pp \rightarrow H) \cdot \frac{56.7}{700} \cdot \frac{m_h^2}{(700 \text{ GeV})^2} \cdot 4B^2(Z \rightarrow l^+l^-) \quad (17)$$

$$\gamma_H \cdot \sigma_R(pp \rightarrow H \rightarrow 4l) \sim \sigma(pp \rightarrow H) \cdot \frac{56.7}{700} \cdot \frac{m_h^2}{(700 \text{ GeV})^2} \cdot 4B^2(Z \rightarrow l^+l^-) \quad (17)$$

- for $\sigma(pp \rightarrow H) \approx \sigma^{\text{ggF}}(pp \rightarrow H) \approx 1180(180) \text{ fb}$

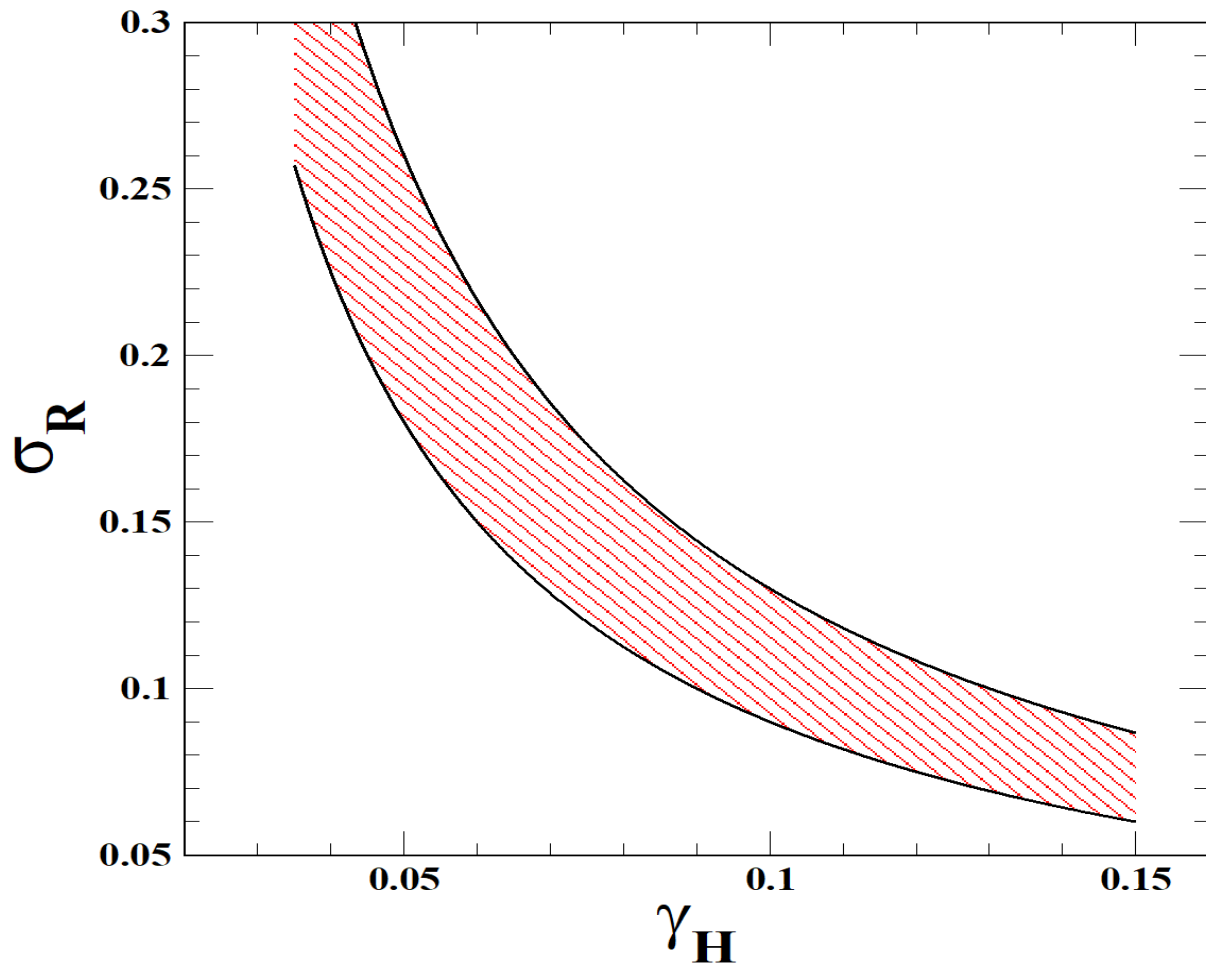
Table 1: We report the ggF cross section in fb to produce a heavy Higgs resonance at $\sqrt{s} = 8$ and 13 TeV. The ratios of the two cross sections, respectively 4.311, 4.393 and 4.477, for $M_H = 660, 680$ and 700 GeV, and the 8 TeV values were taken from the updated Handbook of Higgs cross sections in the CERN yellow report [26]. No theoretical uncertainty is reported.

$M_H[\text{GeV}]$	$\sigma_{\text{gg}}(8 \text{ TeV})$	$\sigma_{\text{gg}}(13 \text{ TeV})$
660	315.3	1359.26
680	268.2	1178.20
700	229.0	1025.23

- $m_h = 125 \text{ GeV}$

$$[\gamma_H \cdot \sigma_R(pp \rightarrow H \rightarrow 4l)]^{\text{theor}} \sim (0.0137 \pm 0.0021) \text{ fb} \quad (18)$$

$$[\gamma_H \cdot \sigma_R(pp \rightarrow H \rightarrow 4l)]^{\text{theor}} \sim (0.0137 \pm 0.0021) \text{ fb} \quad (18)$$



3. Analysis of the ATLAS 4-lepton events

To check the precise correlation in Eq.(18), we have considered the full ATLAS sample [16] of 4-lepton data for luminosity 139 fb^{-1} and in the region of invariant mass $\mu_{4l} = 620 \div 740 \text{ GeV}$ ($l = e, \mu$) which extends about $\pm 60 \text{ GeV}$ around our mass value $M_H = 690 \pm 10 \text{ (stat)} \pm 20 \text{ (sys)} \text{ GeV}$.

Now, Eq.(18) accounts only for production through the ggF mechanism and ignores the VBF-production mode which plays no role in our picture. Therefore, we should compare with that subset of data that, for their typical characteristics, admit this interpretation. To this end, the ATLAS experiment has performed a Multivariate analysis (MVA) of the ggF production mode which combines a multilayer perceptron (MLP) and one or two recurrent neural networks (rNN). The outputs of the MLP and rNN(s) are concatenated so as to produce an event score. In this way, depending on the score, the ggF events are divided into four mutually exclusive categories: ggF-MVA-high- 4μ , ggF-MVA-high- $2e2\mu$, ggF-MVA-high- $4e$, ggF-MVA-low. The four sets of events were extracted from the corresponding HEPData file [27] and are reported in Table 2.

■ Including all ATLAS ggF-like events

Table 2: *At the various 4-lepton invariant mass $\mu_{4l} \equiv E$, we report the ATLAS events for the four different categories of the ggF production mode and their total number.*

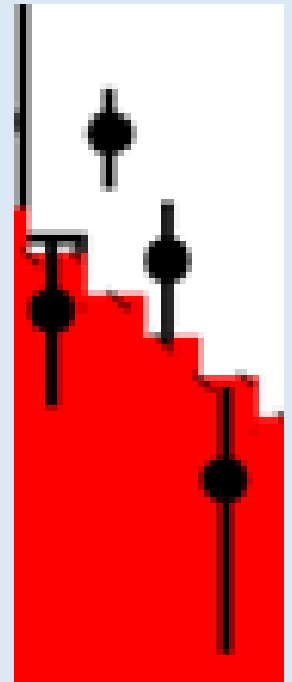
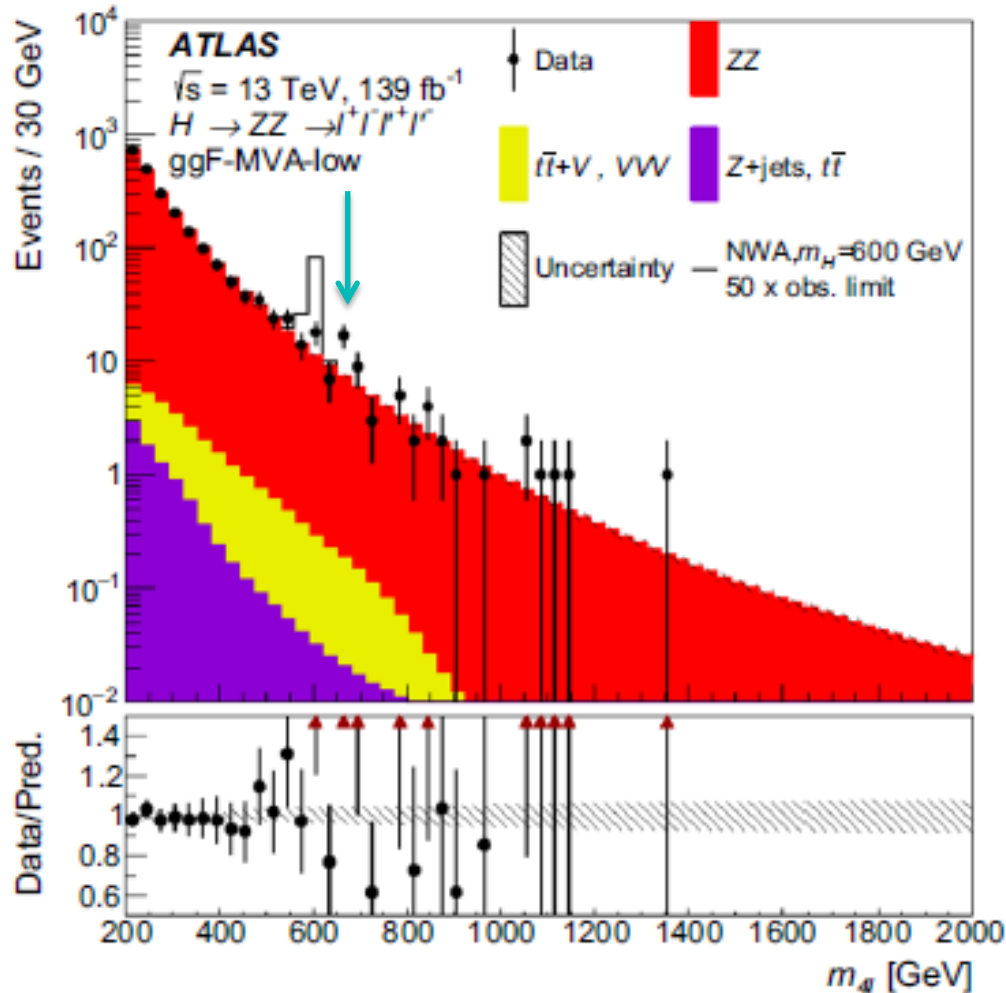
E[GeV]	MVA-high- 4μ	MVA-high- $2e2\mu$	MVA-high- $4e$	MVA-low	ToT
635(15)	2	0	1	7	10
665(15)	0	2	2	17	21
695(15)	1	0	1	9	11
725(15)	0	1	0	3	4

ATLAS 4-lepton events: LUM=139 fb⁽⁻¹⁾

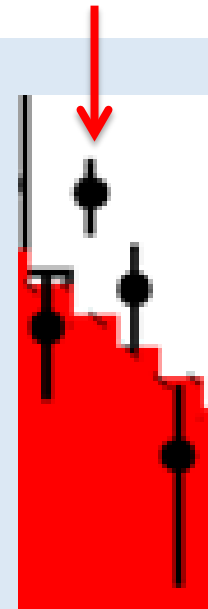
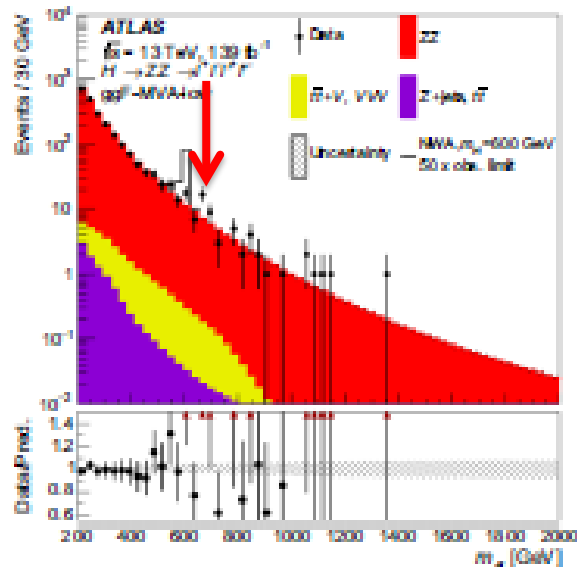
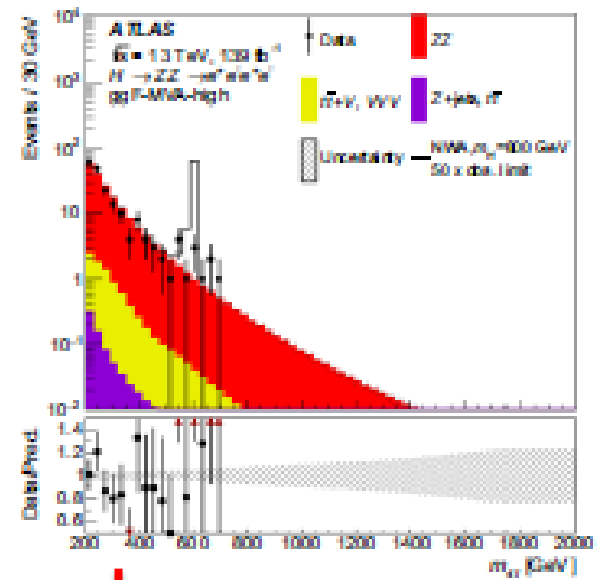
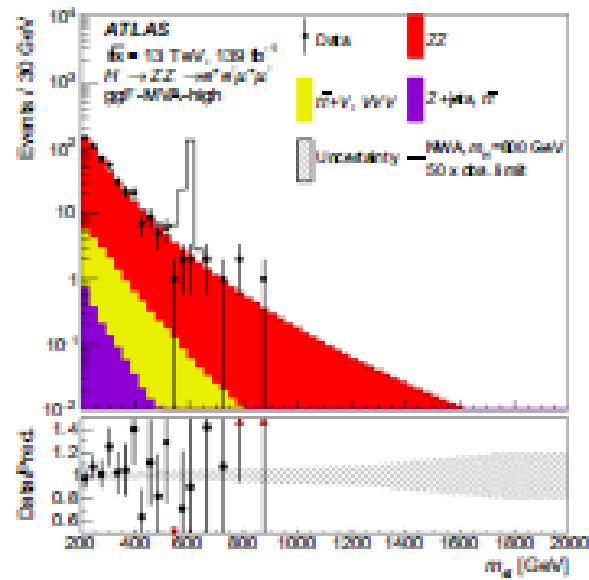
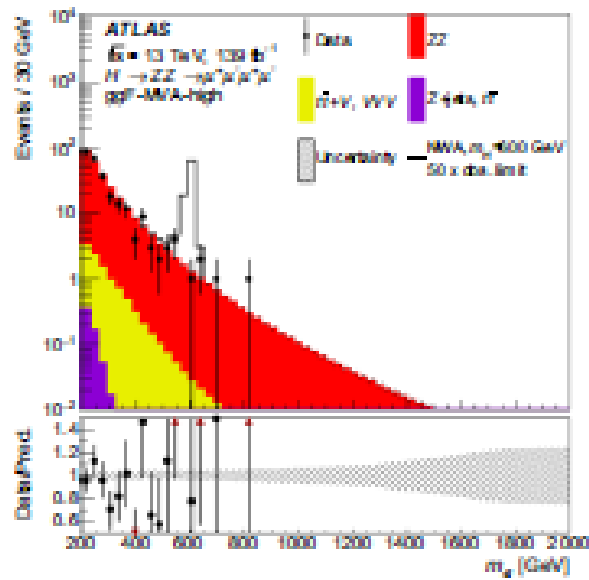
MVA-ggF-low category

$\langle N_{\text{meas}} \rangle = 26(5)$ for $E=650 \div 710$ GeV vs. $N_B \approx 13 \rightarrow 2.6 \sigma$ excess

Relatively narrow resonance at 670(10) GeV (fast decrease of # events)



ATLAS 4-lepton events: LUM=137 fb⁽⁻¹⁾



■ Fitting the ATLAS 4-lepton data in the range 620÷740 GeV

As in refs.[17, 7], by defining $\mu_{4l} = E$ and $s = E^2$, these 4-lepton events will be described by the interference of a resonating amplitude $A^R(s) \sim 1/(s - M_H^2)$ with a slowly varying background $A^B(s)$. For a positive interference below peak, setting $M_R^2 = M_H^2 - iM_H\Gamma_H$, this gives a total cross section

$$\sigma_T = \sigma_B - \frac{2(s - M_H^2) \Gamma_H M_H}{(s - M_H^2)^2 + (\Gamma_H M_H)^2} \sqrt{\sigma_B \sigma_R} + \frac{(\Gamma_H M_H)^2}{(s - M_H^2)^2 + (\Gamma_H M_H)^2} \sigma_R \quad (19)$$

where, in principle, both the average background σ_B , at the central energy 680 GeV, and the resonating peak cross-section σ_R can be treated as free parameters.

Fit to ATLAS data for different $\gamma_H = \Gamma_H/M_H$

Table 3: *For each γ_H we report the values of M_H , the resonating cross section σ_R and the corresponding product $k = \gamma_H \cdot \sigma_R$ which are obtained from a fit with Eq.(19) to the total number of ATLAS events in Table 2.*

γ_H	M_H [GeV]	σ_R [fb]	$k = \gamma_H \cdot \sigma_R$ [fb]
0.05	678(6)	0.218(39)	0.0109(20)
0.06	676(7)	0.191(30)	0.0115(18)
0.07	673(10)	0.174(26)	0.0122(18)
0.08	669(20)	0.161(24)	0.0129(19)
0.09	668(16)	0.151(22)	0.0136(20)
0.10	668(15)	0.141(21)	0.0141(21)
0.11	669(15)	0.133(21)	0.0146(23)
0.12	670(16)	0.125(22)	0.0150(26)
0.13	672(17)	0.118(23)	0.0153(30)
0.14	673(19)	0.112(26)	0.0157(36)
0.15	674(20)	0.106(29)	0.0159(43)

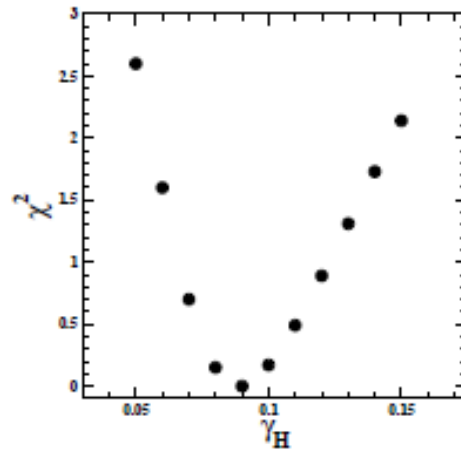


Figure 1: *At the various values of γ_H , we report the chi-square of the fit with Eq.(19) to the ATLAS data.*

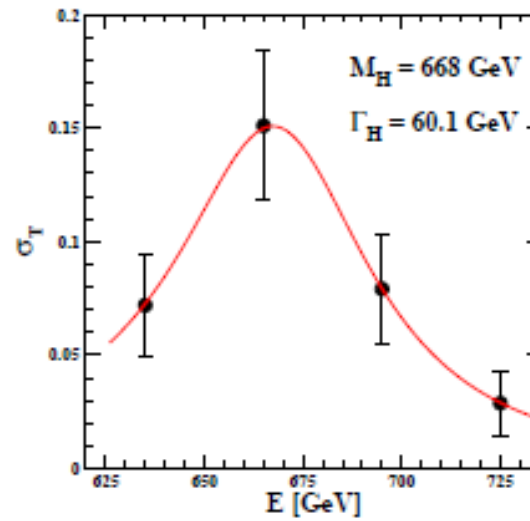


Figure 2: *For $\gamma_H = 0.09$, we show the fit with Eq.(19) to the ATLAS cross sections in fb.*

**Correlation reproduced very well:
excess unlikely to be a statistical fluctuation**

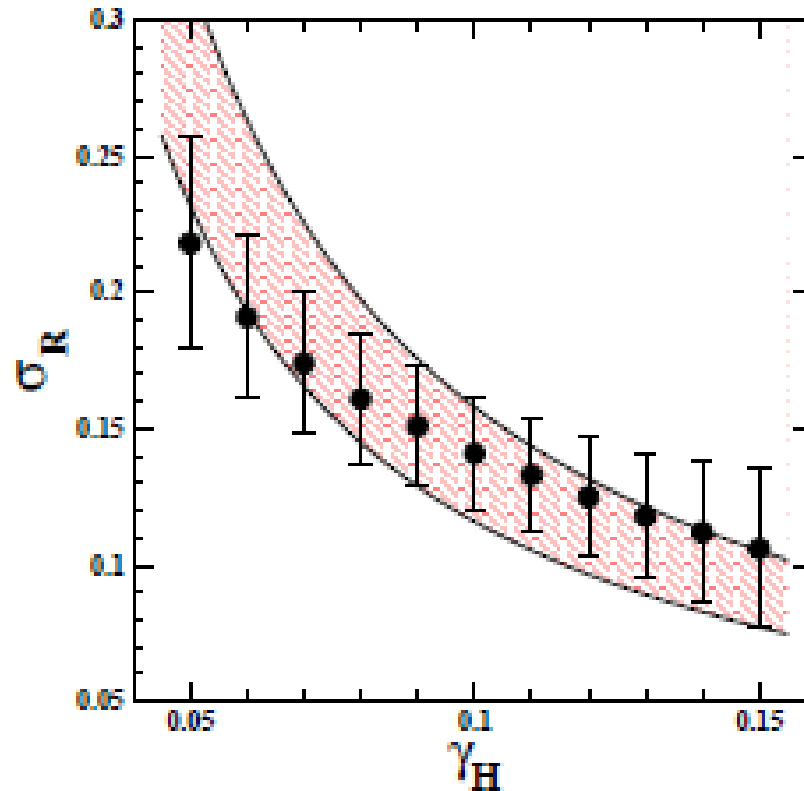
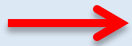


Figure 3: The σ_R 's of Table 3 are compared with our theoretical prediction Eq.(18) represented by the shaded area enclosed by the two hyperbolae $\sigma_R = (0.0137 \pm 0.0021)/\gamma_H$.

Equivalently **one can fit m_h** from the ATLAS 4-lepton data in the high-mass range $620 \div 740$ GeV

γ_H	M_H [GeV]	σ_R [fb]	$k = \gamma_H \cdot \sigma_R$ [fb]
0.05	678(6)	0.218(39)	0.0109(20)
0.06	676(7)	0.191(30)	0.0115(18)
0.07	673(10)	0.174(26)	0.0122(18)
0.08	669(20)	0.161(24)	0.0129(19)
0.09	668(16)	0.151(22)	0.0136(20)
0.10	668(15)	0.141(21)	0.0141(21)
0.11	669(15)	0.133(21)	0.0146(23)
0.12	670(16)	0.125(22)	0.0150(26)
0.13	672(17)	0.118(23)	0.0153(30)
0.14	673(19)	0.112(26)	0.0157(36)
0.15	674(20)	0.106(29)	0.0159(43)

$$\gamma_H \cdot \sigma_R(pp \rightarrow H \rightarrow 4l) \sim \sigma(pp \rightarrow H) \cdot \frac{56.7}{700} \cdot \frac{m_h^2}{(700 \text{ GeV})^2} \cdot 4B^2(Z \rightarrow l^+l^-) \quad (17)$$



$$[\gamma_H \cdot \sigma_R(pp \rightarrow H \rightarrow 4l)]^{\text{theor}} \sim (0.0137 \pm 0.0021) \text{ fb}$$

$$[\gamma_H \cdot \sigma_R(pp \rightarrow H \rightarrow 4l)]^{\text{fit}} = k \sim (0.0137 \pm 0.0008) \text{ fb}$$



$$(m_h)^{\text{fit}} \sim (125 \pm 13) \text{ GeV}$$

- **Some other excess in the same mass region**
 $M = 660 \div 680 \text{ GeV}$

Present CMS 4-lepton data: LUM=137 fb⁽⁻¹⁾

- Relevant data in a single bin 600÷800 GeV.
- No hint on a localized effect near 680 GeV
- Look at lower-statistics samples

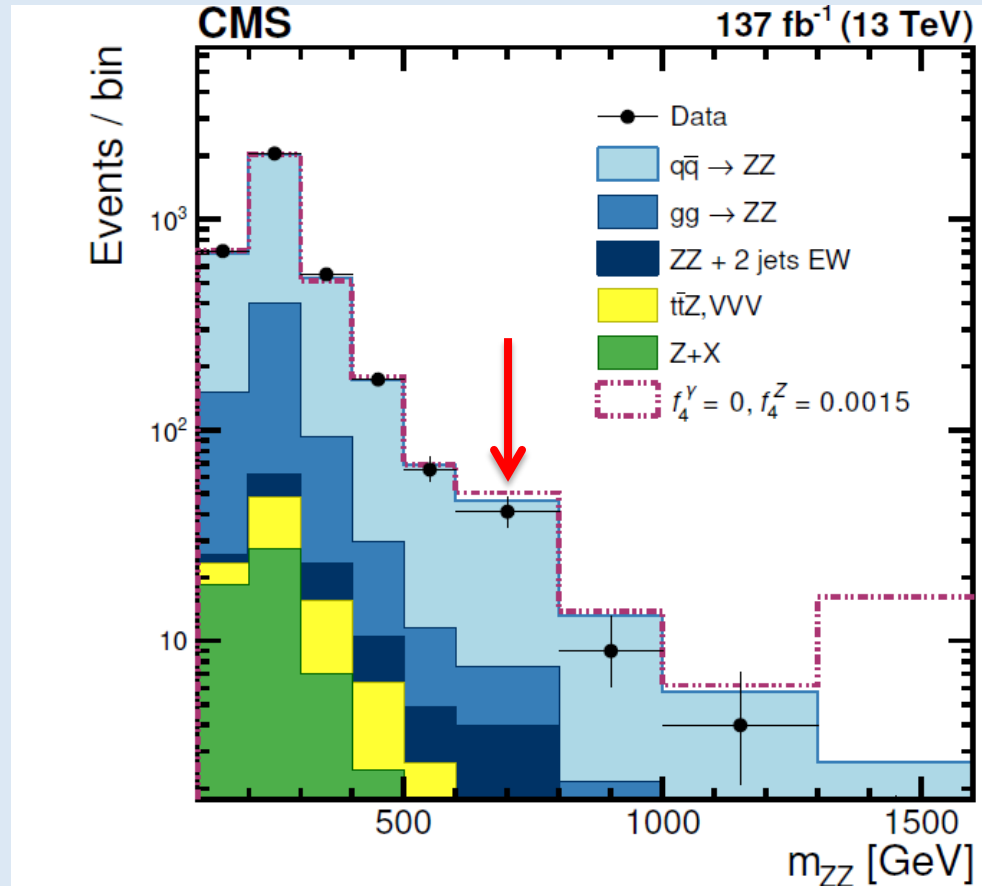


Figure 7: Distribution of the reconstructed ZZ mass for the combined 4e, 2e2 μ , and 4 μ channels. Points represent the data with error bars showing the statistical uncertainties, the shaded histograms represent the SM prediction including signal and irreducible background from simulation, and the reducible background estimate from data. Dashed histogram represents an example of the aTGC signal. The last bin includes contribution from all events with mass above 1300 GeV.

JHEP11(2017)047; arXiv:1706.09936[hep-ex]

CMS 4-lepton 2016 data: Lum=35.9 fb⁽⁻¹⁾

Note: on average 8 events for E=600÷700 GeV vs. 1 event at very end 800 GeV

This is very different from the expected slowly decreasing background.

Sizeable peak at **m(4l)=660(10) GeV** as for ATLAS **m(4l)=665(15) GeV**

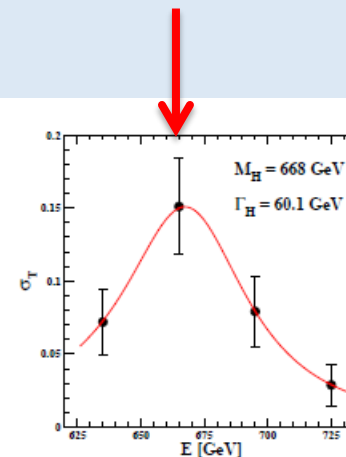
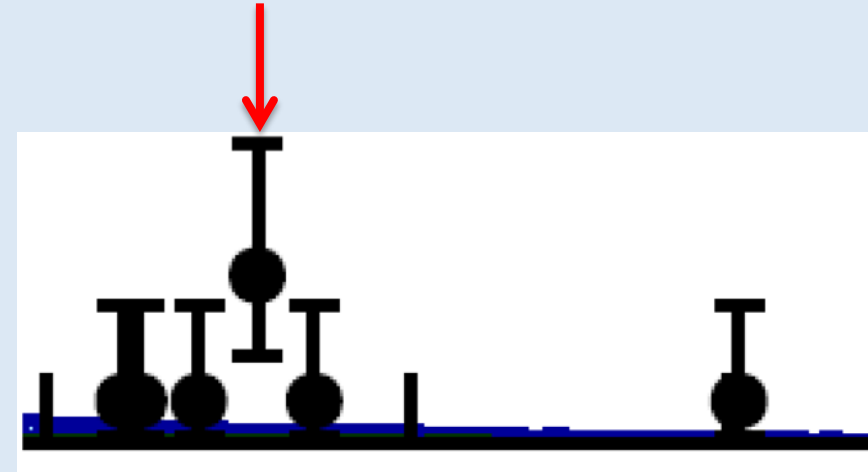
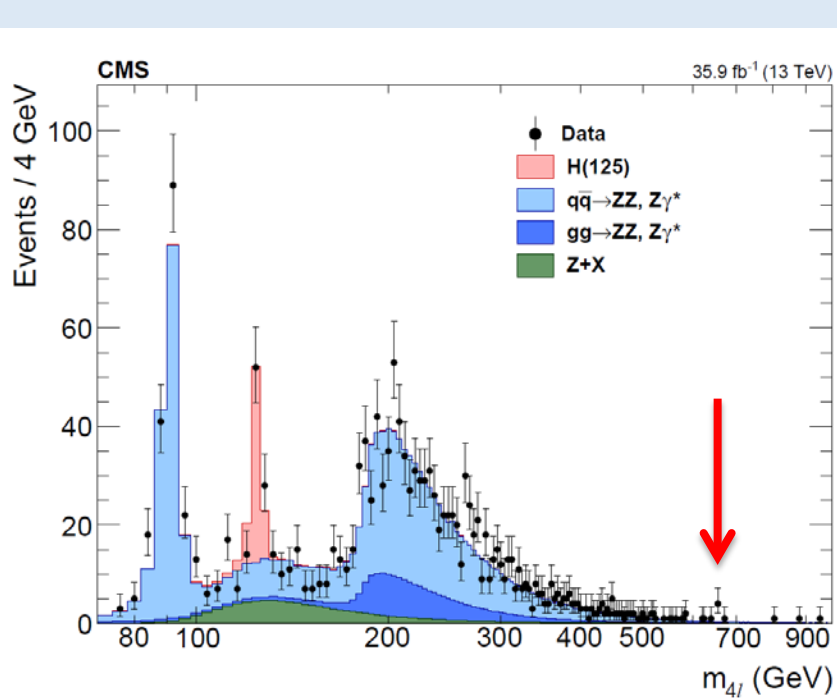
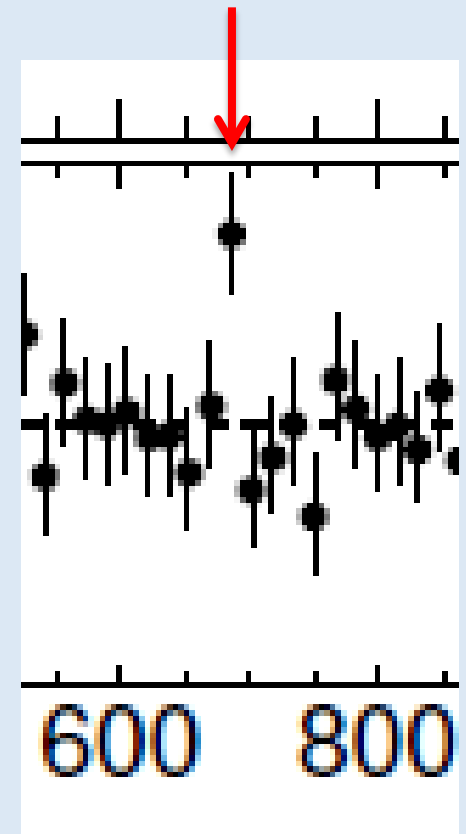
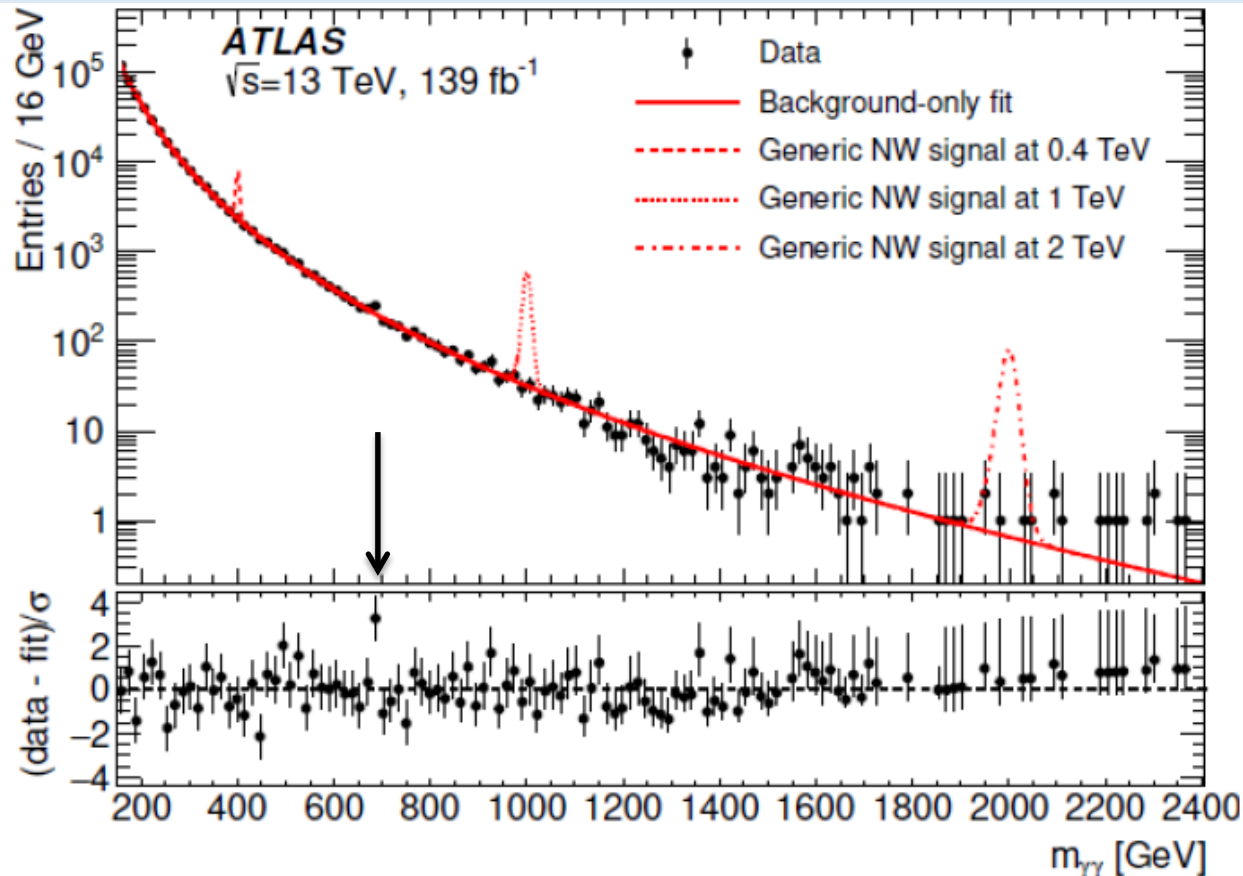


Figure 2: For $\gamma_H = 0.09$, we show the fit with Eq.(19) to the ATLAS cross sections in fb.

ATLAS 2-gamma spectrum:

a (local) 3σ excess at $E=680$ GeV

(here one just sees the interference with the background a + followed by a -)



Rumors (...) about another interesting channel: $H \rightarrow 2b\text{-quark jets} + \gamma\gamma$

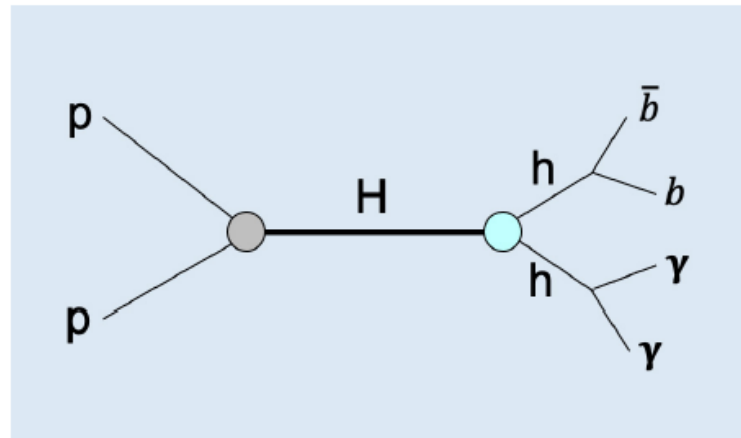


Figure 2: *The production of a final state with 2 b-quark jets + 2 photons through the intermediate heavy state H which then decays into a pair of 125 GeV Higgs bosons. Due to the very large branching ratio $B(h \rightarrow b\bar{b})$ and the clear identification of the 2γ 's this is a particularly interesting channel to look at.*

CONCLUSIONS

- A fit to the ATLAS 4-lepton data points toward a new resonance of mass $(M_H)^{\text{EXP}} = 660 \div 680 \text{ GeV}$
- This value is well consistent with our theoretical prediction for the 2nd resonance of the Brout-Englert-Higgs field $(M_H)^{\text{THEOR}} = 690 \pm 10 \text{ (stat)} \pm 20 \text{ (sys) GeV}$
- By assuming a partial width $H \rightarrow ZZ$ which scales as

$$\Gamma(H \rightarrow ZZ) \sim \frac{M_H}{700 \text{ GeV}} \cdot \frac{m_h^2}{(700 \text{ GeV})^2} 56.7 \text{ GeV}$$

the ATLAS data yield a fitted value $(m_h)^{\text{fit}} = 125 \pm 13 \text{ GeV}$, which reproduces the direct experimental value $(m_h)^{\text{exp}} = 125 \text{ GeV}$

- Our sharp correlation, becomes a guiding principle to trust in other (small) excesses which could be present in other final states.
- The issue of the second resonance could thus be settled now with just the present data from **RUN2**

Interference $H \rightarrow \gamma\gamma$ with non-resonating background (1)

For $s \sim M_H^2$, the total cross section has then the form

$$\sigma_T(s) = \sigma_B(s) + \sigma_R \frac{M_H^2 \Gamma_H^2}{(s - M_H^2)^2 + M_H^2 \Gamma_H^2} + \sqrt{\sigma_R \sigma_B} \frac{2M_H \Gamma_H (M_H^2 - s)}{[(s - M_H^2)^2 + M_H^2 \Gamma_H^2]}$$

From ATLAS Fig.3 in [1], for $\sqrt{s} \sim M_H \sim 680$ GeV and luminosity of 139 fb^{-1} , the background gives about 200 events so that $\sigma_B \sim 1.45 \text{ fb}$.

For the pure ggF-production estimate $\sigma(pp \rightarrow M_H) \sim (1180 \pm 180) \text{ fb}$ (which describes well the ATLAS 4-lepton data), and even by taking into account substantial enhancements of the standard branching fraction (say from $\lesssim 1 \cdot 10^{-7}$ to about $6 \cdot 10^{-6}$), the pure resonating term would be too small to be observed.

$$\sigma_R(pp \rightarrow H \rightarrow \gamma\gamma) \sim \sigma(pp \rightarrow M_H) \cdot B(M_H \rightarrow \gamma\gamma) \leq 0.01 \text{ fb}$$

However, by defining the parameter x through the relation $(M_H - \sqrt{s}) = x\Gamma_H$, and for $x = \pm 1/2$, the interference effect could become visible if

$$\sigma^{\text{int}}(s) \sim \sqrt{\sigma_R \sigma_B} \cdot \frac{4x}{1 + 4x^2}$$

$$\sigma^{\text{int}}(s) \sim [\sigma(pp \rightarrow M_H) \cdot B(M_H \rightarrow \gamma\gamma)]^{1/2} \sqrt{1.45 \text{ fb}} \sim 0.1 \text{ fb}$$

Interference $H \rightarrow \gamma\gamma$ with non-resonating background (2)

$$\sigma^{int}(s) \sim [\sigma(pp \rightarrow M_H) \cdot B(M_H \rightarrow \gamma\gamma)]^{1/2} \sqrt{1.45 fb} \sim 0.1 fb$$

- For $\sigma(pp \rightarrow M_H) \approx \sigma^{ggF}(pp \rightarrow M_H) \approx 1180(180) fb$, this means
- $B(M_H \rightarrow \gamma\gamma) \approx (5 \div 6) \cdot 10^{-6}$ about $(50 \div 60)$ times larger than the estimate 10^{-7} for the standard pair $\Gamma(M_H \rightarrow \gamma\gamma) \approx 18 keV$ and $\Gamma(M_H \rightarrow all) \approx 180 GeV$
- **Here, however, there can be two changes:**
- **i) a total width $\Gamma(M_H \rightarrow all) \approx (40 \div 60) GeV$ (as for the second resonance)**
- **ii) a partial width $\Gamma(M_H \rightarrow \gamma\gamma) \approx (150 \div 200) keV$ (dropping the “-2” non decoupling term as in Gastmans-Wu-Wu & Christova-Todorov computations)**

No more strong cancelation between W loop and top-quark loop. For $M_H = 700 GeV$, and pure 1-loop (i.e. no QCD corrections in the top loop), for $\eta = 0$ or 1 , the width can be expressed as

$$\Gamma_0(M_H \rightarrow \gamma\gamma) \sim 38 keV \left| 1.536 - 2\eta - i \cdot 0.025 \right|^2 \quad (7)$$

and changes from about 8.2 KeV for $\eta = 1$ to about 90 KeV for $\eta = 0$. Besides, QCD corrections are also large for $M_H \sim 700 GeV$.

A remark on radiative corrections

- With two resonances of the Higgs field, what about radiative corrections?
- Our lattice simulations indicate a propagator structure

$$G(p) \sim \frac{1 - I(p)}{2} \frac{1}{p^2 + m_h^2} + \frac{1 + I(p)}{2} \frac{1}{p^2 + M_h^2} \quad (4)$$

with an interpolating function $I(p)$ which depends on an intermediate momentum scale p_0 and tends to $+1$ for large $p^2 \gg p_0^2$ and to -1 when $p^2 \rightarrow 0$.

- This is very close to van der Bij propagator Acta Phys. Polon. B11 (2018) 397.

$$(-1 \leq \eta \leq 1)$$

$$G(p) \sim \frac{1 - \eta}{2} \frac{1}{p^2 + m_h^2} + \frac{1 + \eta}{2} \frac{1}{p^2 + M_H^2} \quad (49)$$

- In the ρ -parameter at one loop, this is similar to have an effective Higgs mass

$$m_{\text{eff}} \sim \sqrt{m_h M_H} (M_H / m_h)^{\eta/2} \quad (47)$$





In our case, this would be between $m_h = 125$ GeV and $M_H \sim 700$ GeV.

- How well, the mass from radiative corrections agree with the direct LHC result 125 GeV?


From the PDG review: positive M_H - $\alpha_s(M_Z)$ correlation (Important: NuTeV is not considered \rightarrow larger M_H)

32 10. Electroweak model and constraints on new physics

Table 10.7: Values of \hat{s}_Z^2 , s_W^2 , α_s , m_t and M_H [both in GeV] for various data sets. In the fit to the LHC (Tevatron) data the α_s constraint is from the $t\bar{t}$ production [204] (inclusive jet [205]) cross-section.

Data	\hat{s}_Z^2	s_W^2	$\alpha_s(M_Z)$	m_t	M_H
All data	0.23122(3)	0.22332(7)	0.1187(16)	173.0 ± 0.4	125
All data except M_H	0.23107(9)	0.22310(19)	0.1190(16)	172.8 ± 0.5	90^{+17}_{-16}
All data except M_Z	0.23113(6)	0.22336(8)	0.1187(16)	172.8 ± 0.5	125
All data except M_W	0.23124(3)	0.22347(7)	0.1191(16)	172.9 ± 0.5	125
All data except m_t	0.23112(6)	0.22304(21)	0.1191(16)	176.4 ± 1.8	125
M_H, M_Z, Γ_Z, m_t	0.23125(7)	0.22351(13)	0.1209(45)	172.7 ± 0.5	125
LHC	0.23110(11)	0.22332(12)	0.1143(24)	172.4 ± 0.5	125
Tevatron + M_Z	0.23102(13)	0.22295(30)	0.1160(45)	174.3 ± 0.7	100^{+31}_{-26}
LEP	0.23138(17)	0.22343(47)	<u>0.1221(31)</u>	182 ± 11	274^{+376}_{-152} 
SLD + M_Z, Γ_Z, m_t	0.23064(28)	0.22228(54)	<u>0.1182(47)</u>	172.7 ± 0.5	38^{+30}_{-21} 
$A_{FB}^{(b,c)}, M_Z, \Gamma_Z, m_t$	0.23190(29)	0.22503(69)	<u>0.1278(50)</u>	172.7 ± 0.5	348^{+187}_{-124} 
$M_{W,Z}, \Gamma_{W,Z}, m_t$	0.23103(12)	0.22302(25)	<u>0.1192(42)</u>	172.7 ± 0.5	84^{+22}_{-19} 
low energy + $M_{H,Z}$	0.23176(94)	0.2254(35)	0.1185(19)	156 ± 29	125

First remark: NuTeV not included by PDG

The NuTeV collaboration found $s_W^2 = 0.2277 \pm 0.0016$ (for the same reference values), which was 3.0σ higher than the SM prediction [89]. However, since then several groups have raised concerns about interpretation of the NuTeV result, which could affect the extracted $g_{L,R}^2$ (and thus s_W^2) including their uncertainties and correlation. These include the assumption of symmetric strange and antistrange sea quark distributions, the electron neutrino contamination from K_{e3} decays, isospin symmetry violation in the parton distribution functions and from QED splitting effects, nuclear shadowing effects, and a more complete treatment of EW and QCD radiative corrections. A more detailed discussion and a list of references can be found in the 2016 edition of this *Review*. The precise impact of these effects would need to be evaluated carefully by the collaboration, but in the absence of a such an effort we do not include the ν DIS constraints in our default set of fits. 

Second remark: the importance of $\alpha_s(M_Z)$

Schmitt → present most complete analysis

hep-ex/0401034
nuhep-exp/04-01

Apparent Excess in $e^+e^- \rightarrow$ hadrons

Michael Schmitt

Northwestern University

January 22, 2004

Abstract

We have studied measurements of the cross section for $e^+e^- \rightarrow$ hadrons for center-of-mass energies in the range 20–209 GeV. We find an apparent excess over the predictions of the Standard Model across the whole range amounting to more than 4σ .

Higgs mass from LEP1

TOKUSHIMA 95-02
(hep-ph/9503288)
March 1995

Remarks on the Value of the Higgs Mass from the Present LEP Data

M. CONSOLI^{a)} AND Z. HIOKI^{b)}

ABSTRACT

We perform a detailed comparison of the present LEP data with the one-loop standard-model predictions. It is pointed out that for $m_t = 174$ GeV the “bulk” of the data prefers a rather large value of the Higgs mass in the range 500-1000

ALEPH+DELPHI+L3+OPAL

α_s	0.113	0.125	0.127	0.130
$m_h(\text{GeV})$	100	100	500	1000
TOTAL χ^2	43.6	37.8	36.4	38.2

Table VII. Total χ^2 for the four Collaborations.

α_s	0.113	0.125	0.127	0.130
$m_h(\text{GeV})$	100	100	500	1000
ALEPH	6.7	8.6	7.6	8.2
DELPHI	7.6	8.8	7.3	7.3
L3	10.3	4.7	5.4	5.9
OPAL	11.4	7.9	5.1	4.1
TOTAL χ^2	36.0	30.0	25.4	25.5

Table VIII. Total χ^2 for the four Collaborations by excluding the data for $A_{FB}^o(\tau)$.